研究症例

8番染色体短腕腕内トリソミー・端部モノソミーの1症例における経時的表現型変化

三井 弓子[*1,2]・中根 貴弥[*1]
林辺 英正[*2]・相原 正男[*3]・中澤 眞平[*4]

要旨

8番染色体短腕腕内トリソミー・端部モノソミーの1例を経験した。同疾患では突き出た額，顎，大きく異常な形をした耳，大きな口，めくれあがった下口唇などの特徴的臨床症状を有するが，これら臨床症状が加齢とともに顕著になることが判明した。

(小児科臨床 56：1613，2003)

KEY WORDS▶ 8番染色体短腕腕内トリソミー・端部モノソミー，FISH 法

緒言

8番染色体短腕腕内トリソミー・端部モノソミーは，現在までに約50例の症例報告がある。比較的稀な染色体構造異常であり，突き出た額，顎，大きく異常な形をした耳，大きな口，めくれあがった下口唇などの特徴的臨床症状を有する。今回，私たちは，学童期から重症心身障害児施設に入所していた成人男性について，臨床症状から染色体異常を疑い，FISH 法により8番染色体短腕腕内トリソミー・端部モノソミーと診断を確定できた。同疾患の長期間にわたる経過観察の報告はなく，貴重であると考えたため，文献的考察を加えて報告する。

症例

症例：28歳，男性（図1）

主訴：特異的顔貌，筋緊張低下，てんかん

現病歴：在胎41週，体重4,400g（+2.63 SD）で吸引分娩により出生した。新生児仮死を認めた。2歳1カ月の時に歩行開始がみられず，有意語もないため，某病院小児科を受診したところ，脳性麻痺と診断された。7歳時に数回のけいれん発作のため近医を受診し，脳波異常（前頭葉から側頭葉を中心に棘波が出現）を指摘され，抗けいれん剤（バルプロ酸，クロナゼパム）の内服を開始した。以後，けいれん発作は1年に数回程度認められている。12歳時に，あけぼの医療福祉センターに入所した。

発達歴：定頸は7カ月，寝返り，這い這いは6歳，独坐はできない。日常生活では，食事，排泄とも全介助が必要である。発声はあるが，有意語の発語は認められない。

家族歴：両親は健康であり，血族結婚では

*1：山梨県立あけぼの医療福祉センター（〒407-0046 山梨県韮崎市旭町上條南割3313-1），*2：山梨大学医学部小児科，*3：同 講師，*4：同 教授

図1　28歳時全身像

図2　12歳時顔正面像
突き出た額，顎，大きく異常な形をした耳，大きな口，めくれあがった下口唇などの特徴的臨床症状は目立たない．

図3　18歳時顔正面像

ない。健康な姉が2人いる。

既往歴：特記事項なし。

身体所見（28歳時；図1）：

体格；身長161cm（−1.21SD），体重31.6 kg，BMI 12.1

顔貌（12歳時；図2，18歳時；図3，28歳時；図4）；突き出た額，顎，大きく異常な形をした耳，大きな口，めくれあがった下口唇などの特徴的臨床症状は，加齢に伴い顕著に認められた。

胸部；肺音は清，心音も整で，心雑音を認めない。

腹部；平坦，かつ軟。下腹部の左右両側に停留睾丸と考えられる直径約5 cm（25mℓ以上）の弾性軟の腫瘤がある。

脊椎・四肢；軽度の側彎を認める。両側下肢に痙性麻痺があり，膝関節の伸展制限がある。

検査所見：検尿，血液生化学一般検査では特別な所見を認めない。

核型；46XY，der（8）dup（8）（p23.1 p12）del（8）（p23.1）ish der（8）（wcp 8＋）

G-banding分析により8番染色体 p23-p12部分の逆位の重複および8番染色体p23.1を切断点とする欠失からなる派生染色体が認められた（図5）。派生染色体の由来が8番染色体であることを whole chromosome painting（wcp）probe 8 による FISH 法により確認した（図6）。

(A) 28歳時顔正面像　　(B) 28歳時顔側面像

図4
12歳時と比較して突き出た顎，突き出た額，大きな耳，分厚い口唇，めくれあがった下口唇といった特徴的臨床症状をより顕著に認める．

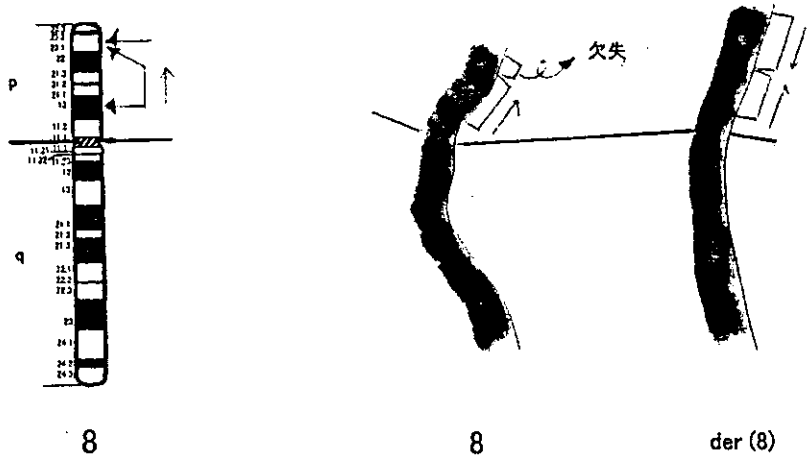

図5　今回の症例で認められた染色体構造異常
G-banding 法の分析で，8番染色体 p23.1-p12部分の逆位の重複および p23.1を切断点とする欠失からなる派生染色体が認められた．

考　察

8番染色体短腕腕内トリソミー・端部モノソミー症例における8番染色体短腕腕内の重複部位は，今回の症例で認められた p12-p23 の他に，p12-p21，p12-p22などが報告されている[1)2)]。Nevin らにより，今回の症例と同様の核型を持った16カ月男児の1例が報告されている[3)]。今回の症例と Nevin らの報告症例で認められる臨床症状，および過去に報告された8番染色体短腕腕内トリソミー・端部モノソミー34例の特徴的臨床症状の出現頻度を表に示す[1)~3)]。今回の症例において，加齢により顕著になった臨床症状，特に突き出

表　8番染色体短腕腕内トリソミー・端部モノソミーの臨床症状

	der(8)dup(8)(p23.1p12)	del(8)(p23.1)	8番染色体短腕腕内トリソミー・端部モノソミー
	今回の症例 28歳	N C Nevin et al 16カ月	過去の報告34例
性　別	男	男	男 17/女 17
出生時体重	4,400g	2,994g	
筋緊張低下	++	+	95.8%
突き出た額，顎	++	+	95.8%
大きく異常な形の耳	++	−	44.1%
大きい鼻中隔	+	−	44.1%
大きな口	+	−	50.0%
めくれあがった下口唇	+	+	55.9%
高口蓋	−	n.d.	52.9%
短い首	+	n.d.	26.5%
側　彎	+	n.d.	62.5%
細い四肢	+	n.d.	26.5%
てんかん	+	n.d.	47.1%
精神発達遅滞	+	+	88.2%

n.d.：記載なし．

図6　FISH法
派生染色体の由来が8番染色体であることを whole chromosome painting (wcp) probe 8により確認した．

た額，顎，大きく異常な形の耳，大きい鼻中隔，大きな口，めくれあがった下口唇は，Nevin らの生後16カ月の症例では軽度である。特徴的臨床症状の出現頻度は，過去に報告された34例において，筋緊張低下，突き出た額，顎は95.8%に認められているが，その他の症状の出現頻度にはばらつきがあり，症例によって奇形の有無や精神運動発達遅滞の重症度に幅がある。8番染色体短腕腕内トリソミー・端部モノソミー症例の欠失部位，重複部位から臨床症状を推測するには更なる症例の集積が必要と思われる。今回の症例は8番染色体 p23-p12部分の逆位の重複および8番染色体 p23.1を切断点とする欠失を有する患者の自然歴を知るうえで示唆深い症例であるといえる。

まとめ

1．FISH 法により診断が確定した8番染色体短腕腕内トリソミー・端部モノソミー症例の幼少期と成人期の臨床症状について報告した。

2．8番染色体短腕腕内トリソミー・端部モノソミー症例で認められる特異顔貌は，加齢により顕著となる。

文　献

1) Antonella M et al：Hum Genet 92：391～396, 1993
2) Moog U et al：Am J Med Genet 94：306～310, 2000
3) Nevin N C et al：J Med Genet 27：135～136, 1990

学会案内

第35回　日本小児感染症学会総会

1．テ　ー　マ：「健やかなこどもの未来のために：たゆまぬ挑戦」
2．会　　長：宮脇　利男（富山医科薬科大学医学部　小児科）
3．会　　期：平成15年11月7日(金)・8日(土)
4．会　　場：富山国際会議場大手町フォーラム，富山全日空ホテル（富山市大手町）
5．参 加 費：8,000円，抄　録　代：2,000円
6．プログラム予定
(1) 招請講演
1)「A role for cytokines/chemokines in EBV-disease pathogenesis」
演者：Giovanna Tosato (NIH/NCI)
2)「Molecular basis of X-linked primary immunodeficiency diseases」
演者：Hans D. Ochs (University of Washington)
(2) 特別講演
「糖鎖からみたインフルエンザ感染」
演者：鈴木　康夫（静岡県立大学薬学部）
(3) 教育講演
1)「小児呼吸器感染症診療のガイドライン」
演者：上原すゞ子（千葉大学・埼玉医科大学小児科）
2)「漢方薬とウイルス感染症」
演者：白木　公康（富山医科薬科大学ウイルス学）
(4) シンポジウム
「これからの院内感染対策」
(5) イブニングセミナー
「ガンマグロブリン療法の今日的意義」
(6) 市民公開講座
「ワクチンとこどもの未来」
(7) 一般演題（ポスターならびに口演）
(8) ランチョンセミナー
7．ホームページアドレス：http://pid35.umin.jp
8．問い合わせ先ならびに学会事務局：〒930-0194　富山市杉谷2630
富山医科薬科大学医学部小児科
金兼弘和・足立雄一
Tel：076-434-7313/Fax：076-434-5029
E-mail：kanegane@ms.toyama-mpu.ac.jp

ELSEVIER

Brain & Development 25 (2003) 195–199

BRAIN & DEVELOPMENT
Official Journal of the Japanese Society of Child Neurology

www.elsevier.com/locate/braindev

Original article

Development of the prefrontal lobe in infants and children: a three-dimensional magnetic resonance volumetric study

Hideaki Kanemura[a], Masao Aihara[a,*], Shigeki Aoki[b], Tsutomu Araki[b], Shinpei Nakazawa[a]

[a]*Department of Pediatrics, School of Medicine, University of Yamanashi, 1110 Shimokato, Tamaho-cho, Yamanashi 409-3898, Japan*
[b]*Department of Radiology, School of Medicine, University of Yamanashi, Yamanashi, Japan*

Received 6 August 2002; received in revised form 20 September 2002; accepted 10 October 2002

Abstract

Relatively little is known about normal prefrontal lobe development. We used three-dimensional magnetic resonance imaging (MRI)-based brain volumetry to characterize developmental changes in prefrontal lobe volumes in infants and children. Prefrontal volumes were determined in 30 subjects aged 5 months to 18 years (221 months) and 3 adults aged 28–39 years (324–468 months). Images were acquired on a 1.5-T MRI system using T1-weighted gradient-echo sequences. Volumes of the frontal and prefrontal lobes were determined using a workstation, and the prefrontal-to-frontal volume ratio was calculated. Prefrontal lobe volume increased slowly until 8 years (96 months) of age, contrasting sharply with rapid growth between 8 and 14 years (96 and 168 months). The prefrontal-to-frontal volume ratio increased with age as a sigmoid growth curve. A prefrontal growth spurt occurs in late childhood. Knowledge of prefrontal lobe development is essential for understanding cognitive development and dysfunction.

Keywords: Three dimensional magnetic resonance imaging; Brain volumetry; Frontal lobe; Prefrontal lobe

1. Introduction

The prefrontal lobe functions in response inhibition, emotional regulation, and planning; prefrontal dysfunction can cause attention deficit/hyperactivity disorder (ADHD) or lack of moral judgment [1–8]. Prefrontal function and its disorders, however, are not immediately apparent, since the prefrontal lobe is among the last cortical regions to reach full structural development [1,9]. Prefrontal functions therefore show an unusually long period of increased vulnerability, in which neurons and glial cells are affected easily by many factors including genetic influences, hormonal milieus, and external insults such as infections, toxins, and trauma [10].

Magnetic resonance imaging (MRI)-based volumetry has become established as a versatile, reliable method for investigating the biology of the human brain [11,12]. Such volumetric analysis has contributed to the search for structural correlates of developmental disorders such as autism and ADHD [13–15]. However, relatively few imaging studies have presented the quantitative measurement of the frontal lobe volumes in infants and children. Furthers, to our knowledge, no attempt has been made to measure development of the prefrontal lobes in this period by imaging until our preliminary three-dimensional (3D) MRI study in 13 children and three adults showing that growth of frontal and prefrontal lobes accelerated during preadolescence [16]. Interpretation of this finding has been limited by the small sample size. Moreover, there was unevenly distributed among the ages of the subjects. Therefore, it was impossible to take statistical analysis. In the present investigation, we studied developmental changes of the frontal and prefrontal lobe volumes in larger group to establish such developmental characteristics of the prefrontal lobe as the prefrontal growth spurt and the growth difference between prefrontal and frontal lobes.

2. Subjects and methods

2.1. Subjects

The study group consisted of 30 children including 22 boys and eight girls, ranging in age from 5 months to 18 years (221 months) (mean, 8 years; 96 months), and also three adults (two men and one woman) aged 28–39 years (324–468 months). All were born at term (37-42 weeks gestational age) following

* Corresponding author. Tel.: +81-55-273-9606; fax: +81-55-273-6745.
E-mail address: maihara@res.yamanashi-med.ac.jp (M. Aihara).

0387-7604/02/$ - see front matter © 2002 Elsevier Science B.V. All rights reserved.
doi: 10.1016/S0387-7604(02)00214-0

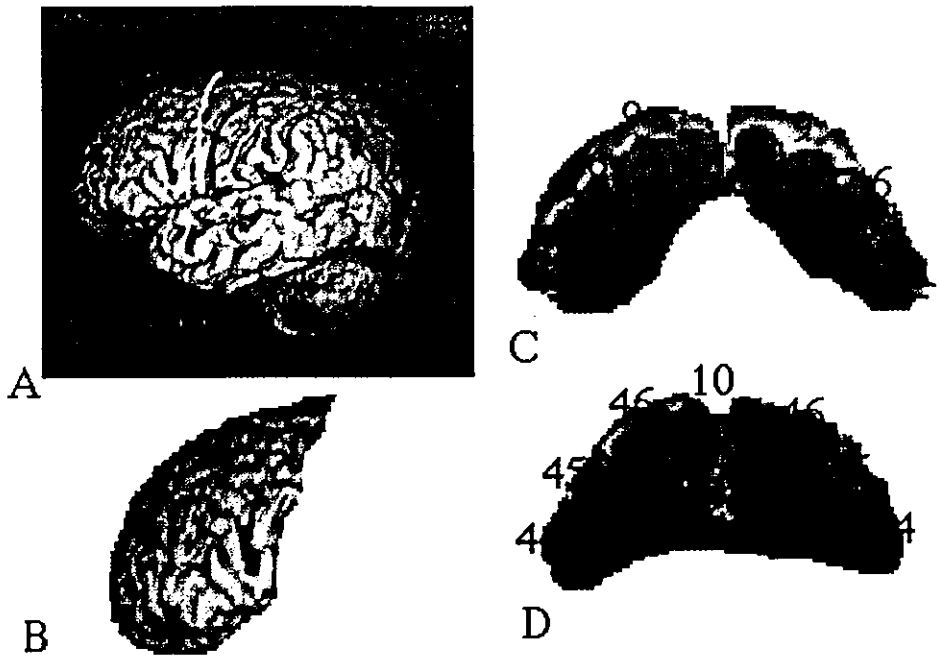

Fig. 1. Three-dimensional (3D) surface and axial views. (A) 3D surface view of the left hemisphere with the central sulcus identified in red and the precentral sulcus in yellow. (B) Regions anterior to the precentral sulcus, with 'erasure' of all voxels posterior to the yellow line. (C,D) Representative images resliced in the axial plane parallel to the anterior and posterior commissure line. Maps of the anatomy were used to compare these axial views with illustrations in the atlas of Damasio and Damasio [18]. Numbers identify Brodmann areas.

uncomplicated prenatal and perinatal courses, and their neurodevelopmental and medical histories were normal. None in school age had received special educational services or private tutoring. None had a history of behavioral or psychiatric disorder. Clinical indications for MRI were followed, i.e. suspected brain trauma, suspected brain tumor, short stature, and migraine; these factors proved to be neurologically and neuropsychologically insignificant during a follow-up period of 2–4 years after MRI. No subject had abnormal findings by routine MRI. Informed consent was obtained from the subjects and their parents.

2.2. Image acquisition and processing

All MRI was performed on a 1.5-T Signa unit (General Electric, Milwaukee, WI). The 3D MRI data were acquired by fast spoiled-gradient recalled echo in a steady state with 3D Fourier transformation. Contiguous 1.0–1.2-mm slices were obtained through the head (flip angle, 30°; matrix size, 256 × 256; TR, 14.5 ms; TE, 4.5 ms; field of view, 18 × 18 to 22 × 22 cm). Using an Advantage Windows RP 3D analyzer (General Electric), 3D images of the brain surface were generated from the 124 MRI slices. Next, the central and precentral sulcus were identified in left and right lateral as well as superior 3D views of the brain surface, according to boundaries described by Ono et al. [17]. The frontal and prefrontal lobes were determined as the regions anterior to the central and precentral sulcus, respectively. We also confirmed frontal and prefrontal lobe extent by comparison of scans with images resliced in the axial plane parallel to the anterior and posterior commissure (AC-PC) line, using the standardized stereotaxic atlas of Damasio and Damasio [18]. Finally, we measured the frontal and prefrontal lobe volumes by the volume measurement function of the workstation based on the 3D images.

To confirm the reliability of workstation functions, we compared the whole-brain volume calculated from 3D data with directly measured volumes for three cadaver brain specimens. To assess intra-rater, inter-trial reliability all images were remeasured 2 weeks after the first measurement. Ten images were chosen randomly to assess inter-rater reliability.

2.3. Statistical analysis

Pearson's correlation coefficient was used to assess inter-observer agreement and intra-rater, inter-trial reliability. For statistical interpretation of growth patterns, nonlinear regression analysis was performed. The equation chosen for curve-fitting was a cubic equation representing a sigmoid growth function.

3. Results

3.1. 3D brain surface images and frontal and prefrontal lobe determinations

Fig. 1A shows a 3D surface view of the left hemisphere with the central sulcus identified as red and the precentral

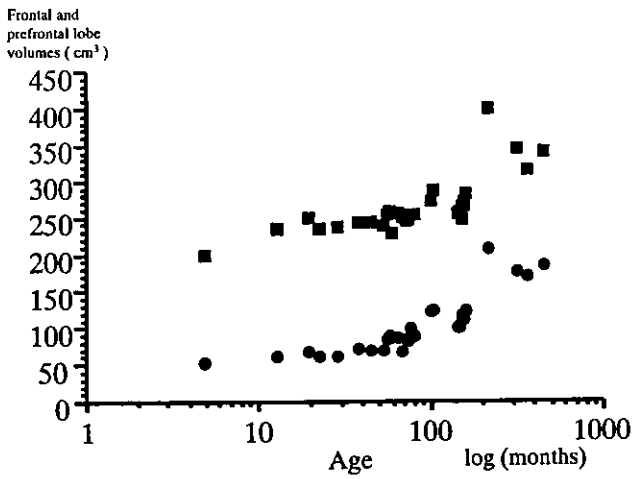

Fig. 2. Developmental changes in frontal and prefrontal lobe volumes. Scatter plots by age of volumes of frontal (squares) and prefrontal (circles) lobes for infant, children, and adults.

sulcus as yellow. In Fig. 1B, only areas anterior to the precentral sulcus are shown, with elimination of all voxels posterior to this sulcus. The representative images resliced in the axial plane parallel to the AC-PC line are shown in Fig. 1C,D. Using the atlas of Damasio and Damasio [18], anatomic regions corresponding to Brodmann areas in these images were determined precisely. The 'prefrontal lobe' in this study was defined as the regions anterior to the yellow line, including the prefrontal lobe proper (Brodmann areas 8, 9, 10, 11, 12, 13, 44, 45, 46, and 47) plus anterior regions of Brodmann area 6, the corpus callosum, and the cingulate gyrus.

3.2. Reliability: workstation, intra-rater and inter-rater

Directly measured volumes of whole brains ranged from 869 cm^3 to 1163 cm^3. The error range for the volumes calculated from 3D MRI for these brains was 0.17–2.02%

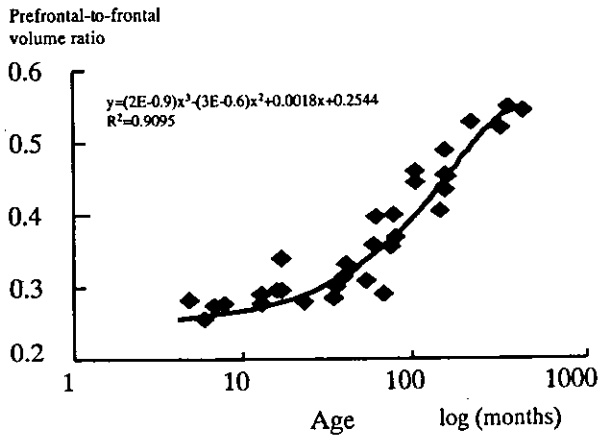

Fig. 3. Developmental changes in prefrontal-to-frontal volume ratios. Scatter plots by age of prefrontal-to-frontal volume ratios for infants, children, and adults.

[16]. Correlation was strong ($P < 0.001$) between directly measured and calculated volumes. Inter-rater correlation coefficient for measurements of ten randomly chosen frontal lobes was 0.87, while the intra-rater correlation coefficient for all cases was 0.98.

3.3. Volumetric measurements of the frontal and prefrontal lobes

Measured volumes for frontal and prefrontal lobes are shown in Fig. 2. Frontal lobe volumes increased steadily with advancing age until age of 10 years (120 months), continuing to increase slowly thereafter. Prefrontal lobe volumes, on the other hand, increased slowly until the age of 8 years (96 months), contrasting sharply with rapid growth between 8 and 14 years (96 and 168 months) to reach completion at about age 18 years (216 months).

3.4. Prefrontal-to-frontal lobe volume ratio

Prefrontal-to-frontal volume ratio as a function of age is shown in Fig. 3, with a slow increase until the age of 8 years (96 months) and a sigmoid curve between 8 and 14 years (96 and 168 months), after which an adult ratio was reached.

4. Discussion

This study established that both frontal and prefrontal lobe volumes consistently increased during childhood and adolescence. Moreover, differential growth of the prefrontal lobe relative to the frontal lobe resulted in an increase in the volume ratio of the prefrontal to frontal lobe that continued until adolescence. Accordingly, the prefrontal cortex is one of the last cortical regions to reach full structural development. We had anticipated such preponderance of volume increase in the prefrontal lobe based on phylogenetic comparisons of relative prefrontal surface areas, such as for humans versus primates [1]. To our best knowledge, this study is the first to show developmental progression and completion of growth in the human prefrontal lobes.

The reliability of MRI-based volumetric analysis stems from advances both in imaging and image analysis [11,19,20]. Performance of fast spoiled gradient-recalled echo imaging in the steady state permits rapid acquisition and 3D volumetric calculations. Very thin contiguous images through the brain can be obtained in a relatively short time without compromising the signal-to-noise ratio [21]. Anatomically reliable identification of the central and precentral sulci is easy with these methods. Past MRI analyses of the size of structures have used manual tracing of structures presented in single planes to estimate a structure's area in the section.

Accuracy of an MRI-based technique for volumetric measurement such as ours is another important issue. We found a high degree of accuracy comparing direct and MRI volumetric measurements in cadaver brains. The mean

percentage error of calculated volumes compared with actual volumes was 0.85%, which was no less accurate than in previous reports in which mean error range was 2.33–3.4% [22,23]; we also obtained a strong statistical correlation between the two methods of measurement ($P < 0.0001$). Furthermore, intra- and inter-rater variation was comparable to those in other studies [24].

In our sample of three adults, mean frontal and prefrontal lobe volumes by our method (averaging the two trials by one rater) were 338.1 ± 15.5 cm^3 and 180.8 ± 6.5 cm^3, respectively. This mean frontal lobe volume was almost the same as reported by Aylward et al. [24] and Andreasen et al. [25] for healthy control subjects, respectively based on surface landmarks (366 ± 23 cm^3) and stereotactic brain-warping (387 ± 50 cm^3). Though no reliable sulcal landmarks exist to measure the size of the prefrontal lobe proper after exclusion of premotor, supplementary motor, and limbic cortices, our mean volume for the prefrontal lobe was close to that obtained by another investigator who examined a subsection of the frontal cortex that included all prefrontal cortices [26]. Thus, using the above method for measurement of the frontal and prefrontal lobe in MRI was considered appropriate for comparison between infants and adults. While a close relationship, best represented by a hyperbolic function, has been shown between brain weight and body weight throughout growth and maturation, comparing prefrontal-to-frontal lobe volume ratios eliminates need to correct measurements for body weight [27].

The size of brain structures directly reflects number, shape, pattern of arrangement, and densities of different cellular components, specifically neurons and glial cells. In normal brain development, which involves overproduction and then selective elimination of neurons through apoptosis, glia cells outnumber neurons and undergo a constant cycle of cell proliferation and death [28]. One glial cell activity is myelination by oligodendrocytes. Postmortem studies indicate that myelination begins in utero in the second trimester and continues well into the third decade of life; the frontal lobes are the last to myelinate [29]. According to a recent longitudinal MRI study, amount of gray matter in the frontal lobe increased to a maximum during pre-adolescence, followed by a decline after adolescence. In contrast, the volume of white matter increased in a linear manner with age from 4 to 20 years [28]. Other investigators reported an increase in prefrontal white matter volume ($P < 0.01$) with increasing age (4–18 years) [30]. These findings supported the hypothesis that increases in myelination in the first and second decades of life are primarily responsible for determining the volume of the prefrontal lobe. During certain phases of rapid brain growth, neurons and glial cells are affected by many factors including genetic influences, hormonal milieus, nutrition, and other external conditions [10]. Our findings that prefrontal growth spurts occur during adolescence and limited periods before and afterward may predict that those periods are not only critical for cognitive development concerning response inhibition, emotional regulation, and planning but also are period of vulnerability to structural damage that may cause developmental disorders.

Recent evidence from electrophysiologic studies and positron-emission tomography studies indicates relatively late frontal maturation [31]. The prefrontal cortex has a well-known functional role in working memory [32]. As a result, neuropsychologic studies show that performance of delayed tasks does not attain full development until adolescence [33]. Fuster [2] postulates that the prefrontal cortex is critical for the temporal organization of goal-directed actions, which involves three cognitive functions: attention, short-term memory, and planning. These cognitive components develop gradually, with spurts between 5 and 10 years of age, reaching completion at post-adolescence [1]. These observations suggest that both MR volumetric and neuropsychologic studies can detect disturbances in form/function relationships in the prefrontal lobe, providing ways of assessing prefrontal development.

Quantification of normal prefrontal lobe volume as in our study is a useful way to characterize excessive deviation in prefrontal lobe size. The maturation-associated changes detectable during development will be important for comparison with maturational sequences in developmental disorders. According to Fuster [2], empirical evidence suggests that early frontal lesions can result in deficits not immediately apparent but predisposing to later developmental problems such as learning disabilities, ADHD, emotional instability, lack of moral judgment, and even criminal behavior. Volumetric analysis of the developing brain, especially the frontal and prefrontal lobes, may predict function in corresponding regions.

Ongoing investigation of these and other issues in our laboratory include analysis of gender-associated differences in right-left asymmetry in the prefrontal lobe [34,35], as well as longitudinal analysis with serial MRI in children who have experienced insults such as hypoxic-ischemic brain damage, malnutrition [36], congenital infection, hormonal disorders, and effects of chromosomal anomalies.

5. Conclusion

Using MRI-based volumetry, we established developmental characteristics of the prefrontal lobe, including a prefrontal growth spurt in late childhood and a growth difference between the prefrontal lobe and the remainder of the frontal lobe. Enhanced knowledge of prefrontal lobe development from birth to adulthood is essential for understanding cognitive development and dysfunction.

Acknowledgements

The authors thank Professor Saoko Atsumi and Toyoko Kawate for use of the cadaver brains.

References

[1] Fuster JM. The prefrontal cortex – anatomy, physiology and neuropsychology of the frontal lobe. 3rd ed. Philadelphia, PA: Lippincott-Raven, 1997. pp. 6–11.

[2] Fuster JM. The prefrontal cortex-an update: time is of the essence. Neuron 2001;30:319–333.

[3] Fuster JM, Bondner M, Kroger JK. Cross-modal and cross- temporal association in neurons of frontal cortex. Nature 2000;405:347–351.

[4] Barkley RA, Grodzinsky G. Are tests of frontal lobe function useful in the diagnosis of attention deficit disorders. Clin Neuropsychol 1994;8:121–139.

[5] Barkley RA. Genetics of childhood disorders: XVII. ADHD, Part 1: the executive functions and ADHD. J Am Acad Child Adolesc Psychiatry 2000;39:1064–1068.

[6] Anderson SW, Bechara A, Damasio H, Tranel D, Damasio AR. Impairment of social and moral behavior related to early damage in human prefrontal cortex. Nat Neurosci 1999;2:1032–1037.

[7] Damasio AR. The somatic marker hypothesis and the possible functions of the prefrontal cortex. Philos Trans R Soc Lond Ser B Biol Sci 1996;351:1413–1420.

[8] Bechara A, Damasio AR, Damasio H, Anderson SW. Insensitivity to future consequences following damage to human prefrontal cortex. Cognition 1994;50:7–15.

[9] Yakovlev PI, Lecours AR. The myelogenetic cycles of regional maturation of the brain. In: Minkowski A, editor. Regional development of the brain in early life, Oxford: Blackwell, 1967. pp. 3–70.

[10] Dobbing J, Sands J. Vulnerability of developing brain: the effect of nutritional growth retardation on the timing of the brain growth spurt. Biol Neonate 1971;19:363–378.

[11] Caviness Jr VS, Lange NT, Makris N, Herbert MR, Kennedy DN. MRI-based brain volumetrics: emergence of a developmental brain science. Brain Dev 1999;21:289–295.

[12] Whitwell JL, Crum WR, Watt HC, Fox NC. Normalization of cerebral volumes by use of intracranial volume: implications for longitudinal quantitative MR imaging. Am J Neuroradiol 2001;22:1483–1489.

[13] Courchesne E, Yeung-Courchesne R, Press GA, Hesselink J, Jernigan T. Hypoplasia of cerebellar vermal lobules VI and VII in autism. N Engl J Med 1988;318:1349–1354.

[14] Piven J, Saliba K, Bailey J, Arndt S. An MRI study of brain size in autism: the cerebellum revisited. Neurology 1997;49:546–551.

[15] Castellanos FX, Giedd JN, Marsh WL, Hamburger SD, Caituzus AC, Dickstein DP, et al. Quantitative brain magnetic resonance imaging in attention-deficit hyperactivity disorder. Arch Gene Psychiatry 1996;53:607–616.

[16] Kanemura H, Aihara M, Aoki S, Hatakeyama S, Kamiya Y, Ono C, et al. Quantitative measurement of prefrontal lobe volumes on three dimensional magnetic resonance imaging scan (in Japanese). No To Hattatsu (Tokyo) 1999;31:519–524.

[17] Ono M, Kubic S, Abernathey CD. Atlas of the cerebral sulci. New York: Thieme Medical Publishers, 1990.

[18] Damasio H, Damasio AR. Lesion analysis in neuropsychology. New York: Oxford University Press, 1989.

[19] Caviness Jr VS, Filipek PA, Kennedy DN. Magnetic resonance technology in human brain science: blueprint for a program based upon morphometry (review). Brain Dev 1989;11:1–13.

[20] Caviness Jr VS, Kennedy DN, Makris N, Bates J. Advanced application of magnetic resonance imaging in human brain science. Brain Dev 1995;17:399–408.

[21] Barkovich AJ. Pediatric neuroimaging. 3rd ed. Philadelphia, PA: Lippincott Williams and Wilkins, 2000. pp. 4–5.

[22] Ashtari M, Zito JL, Gold BI, Lieberman JA, Borenstein MT, Herman PG. Computerized volume measurement of brain structure. Invest Radiol 1990;25:798–805.

[23] Iwasaki N, Hamano K, Okada Y, Horigome Y, Nakayama J, Taketa T, et al. Volumetric quantification of brain development using MRI. Neuroradiology 1997;39:841–846.

[24] Aylward EH, Augustine ALQ, Lia Barta PE, Pearlson GD. Measurement of frontal lobe volume on magnetic resonance imaging scans. Psychiatry Res 1997;75:23–30.

[25] Andreasen NC, Rajarethinam R, Cizadlo T, Arndt S, Swayne Jr VW, Flashman LA, et al. Automatic atlas-based volume estimation of human brain regions from MR images. J Comput Assist Tomogr 1996;20:98–106.

[26] Semendeferi K, Lu A, Schenker N, Damasio H. Humans and great apes share a large frontal cortex. Nat Neurosci 2002;5:272–276.

[27] Dekaban AS, Sadowsky D. Changes in brain weights during the span of human life: relation of brain weights to body heights and body weights. Ann Neurol 1978;4:345–356.

[28] Jernigan TL, Trauner DA, Hesselink JR, Tallal PA. Maturation of human cerebrum observed in vivo during adolescence. Brain 1991;114:2037–2049.

[29] Mrzljak L, Uylings HBM, Van Eden CG, Judas M. Neuronal development in human prefrontal cortex in prenatal and postnatal stages. In: Uylings HBM, Van Eden CG, De Bruin JPC, Corner MA, Feenstra MGP, editors. Progress in brain research, vol. 85. New York: Elsevier Science, 1990. pp. 185–222.

[30] Giedd JN, Snell JW, Lange N, Rajapaskse JC, Casey BJ, Kozuch PL, et al. Quantitative magnetic resonance imaging of human brain development: ages 4–18. Cereb Cortex 1996;6:551–560.

[31] Takahashi T, Shirane R, Sato S, Yoshimoto T. Developmental changes of cerebral blood flow and oxygen metabolism in children. Am J Neuroradiol 1999;20:917–922.

[32] Baddeley A. Working memory. New York: Oxford University Press, 1986.

[33] Piaget J. The origins of intelligence in children. New York: International Universities Press, 1952.

[34] Xu J, Kobayashi S, Yamaguchi S, Iijima K, Okada K, Yamashita K. Gender effects on age-related changes in brain structure. Am J Neuroradiol 2000;21:112–118.

[35] Kanemura H, Aihara M, Nakazawa S. Measurements of the frontal and prefrontal lobe volumes by three dimensional magnetic resonance imaging scan – III. Analysis of sex differences with advanced age(in Japanese). No To Hattatsu (Tokyo) 2002;34:404–408.

[36] Kanemura H, Aihara M, Nakazawa S. Measurement of the frontal and prefrontal lobe volumes in children with malnutrition by three dimensional magnetic resonance imaging scan (in Japanese). No To Hattatsu (Tokyo) 2002;34:398–403.

ELSEVIER

Brain & Development 25 (2003) 555–559

BRAIN & DEVELOPMENT
Official Journal of the Japanese Society of Child Neurology

www.elsevier.com/locate/braindev

Original article

Age shifts frontal cortical control in a cognitive bias task from right to left: part I. Neuropsychological study☆

Masao Aihara[a,*], Kakurou Aoyagi[a], Elkhonon Goldberg[b], Shinpei Nakazawa[a]

[a]*Department of Pediatrics, Faculty of Medicine, University of Yamanashi, 1110 Tamaho-cho, Nakakomagun, Yamanashi 409-3898, Japan*
[b]*Department of Neurology, New York University School of Medicine, New York, NY, USA*

Received 29 January 2003; received in revised form 7 March 2003; accepted 7 March 2003

Abstract

Two functionally and neurally distinct cognitive selection mechanisms involve the prefrontal lobes: those based on internal representations (context dependent) and those involving exploratory processing of novel situations (context independent). We used a cognitive bias task (CBT) representing contextual reasoning to correlate lateralization with age in the frontal lobes. Subjects included 37 healthy right-handed male children and adolescents (age range, 5–18 years). Controls were 19 right-handed men from 20 to 30 years old. A computer-presented version of the original card-choice task simplified, modified for children was used (modified CBT; mCBT). Simple visual stimuli differed dichotomously in shape, color, number, and shading. A target object presented alone was followed by two choices from which subjects selected according to preference. Considering all four characteristics, similarity between target and subject choice was scored for 30 trials. A high score implied a context-dependent response selection bias and a low score, a context-independent bias. Similarity increased significantly with age. The youngest children (5–7 years) scored lower than ages from 11 years to adulthood. Between 7 and 9 years, scores began to increase with age to reach an adult level by age 13–16. Young children showed context-independent responses representing right frontal lobe function, while adolescents and adults showed context-dependent responses implicating left frontal lobe function. The locus of frontal cortical control in right-handed male subjects thus shifts from right to left as cognitive contextual reasoning develops.

Keywords: Cognitive bias task; Context-dependent reasoning; Prefrontal lobe function; Lateralization; Handedness

1. Introduction

The prefrontal cortex, which is critical for the temporal organization of cognitive processes, is among the last cortical regions to reach full functional maturity [1,2]. Prefrontal functions therefore show an unusually long period of vulnerability in which neurons and glia are affected easily by internal and external insults [3]. Furthermore, early frontal lesions can result in deficits not immediately apparent but predisposing to later developmental problems such as learning disabilities, attention deficit/hyperactivity disorder (ADHD), and even problems with moral judgment [4,5]. To fully appreciate the implications of developmental problems in children with the frontal lobe damage, hypothesis-driven studies are needed to explore functions such as working memory or inhibition during childhood, instead of sole reliance on traditional intelligence tests.

Some researchers have hypothesized two functionally and neurally distinct cognitive selection mechanisms involving the prefrontal lobes: those involving processing based on internal representations, e.g. planning (context-dependent reasoning) and those involving exploratory processing of novel cognitive situations (context-independent reasoning) [6–8]. Goldberg et al. recently have refined a cognitive bias task (CBT) for use as an activation procedure representing contextual reasoning, concluding that extreme context-dependent and context-independent response selection biases are respectively linked to left and right frontal systems in right-handed male-subjects [9–11]. On the basis of these findings, we used the CBT to explore development of lateralization in the frontal lobes as a function of age.

Part II: Shimoyama et al. will be published in volume 26, doi: S0387-7604(03)00092-5.

* Corresponding author. Tel.: +81-55-273-9606; fax: +81-55-273-6745.
E-mail address: maihara@res.yamanashi-med.ac.jp (M. Aihara).

0387-7604/03/$ - see front matter © 2003 Elsevier B.V. All rights reserved.
doi:10.1016/S0387-7604(03)00064-0

2. Methods

2.1. Subjects

Subjects included 37 healthy children and adolescents (all male; age range, 5–18 years), and 19 men aged from 20 to 30 years who served as controls. Subjects were evaluated for handedness using Chapman's inventory [12]; all were found to be right-handed, having a score of 17 or less. Informed consent was obtained from subjects and/or their parents.

2.2. Task design

A modified version of the original task developed in 1994 by Goldberg et al. [9] was designed for children (modified CBT; mCBT). Computer-presented 'cards' in the mCBT differed dichotomously in four respects: shape (circle vs. square), color (red vs. blue), number (one vs. two), and shading (outline only vs. homogeneously filled). Thus, 16 different stimuli can be presented. A trial involved presentation of the target card alone, followed by two choice cards below it (Fig. 1). An investigator instructed the subject to look at the target and then select the choice that he preferred. The 30 trial sequences that followed were the same for all subjects. Before presentation of the target card, subjects either read or listened to the following instructions (a Japanese version of Goldberg's instructions: "You will see cards with different designs. The designs may vary in several respects. You will see one card at the top and two cards below it. Look at the top card and choose one of the two cards below that you like the best. There are no correct or incorrect responses. Your choice is entirely up to you. Please try to make your choices quickly. Do you have any questions?").

An index of similarity to the target designed never to be equal between the two choices offered was determined for the subject's choice in each trial, which would be 4 for identical stimuli and range to 0 for stimuli differing in all four possible respects. All interchoice similarity index and target-to-choice similarity index values were equally represented and counterbalanced through the trial sequence. The mCBT raw score was the sum of similarity indices across trials, designed to range from 30 to 90. High and low raw scores implied consistently similar choices—a target-driven selection bias. A middle-range score (around 60) implied that choices were unrelated to corresponding targets (indifferent selection bias). The converted mCBT score was computed as the absolute value of the deviation of the raw score from the midpoint of the raw-score scale, equal to 60. On the converted scale, ranging from 0 to 30, a high score implied a context-dependent response selection bias and a low score, a context-independent bias, irrespective of direction of deviation from the midpoint.

Furthermore, to establish that age influences response bias rather than simply ability to perform the CBT, two control tasks with explicit 'choose the most similar' or 'different' instructions were administered after the mCBT. Finally, subjects were asked to select one of the two choice cards at random without presentation of a target card.

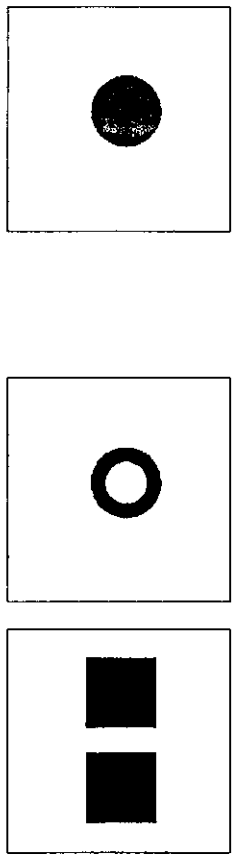

Fig. 1. Example of a cognitive bias task trial. A trial involves presentation of the target alone, with two choices immediately added below the target in vertical alignment. Here, if a subject selects the upper choice as his preference, the similarity index would be 3 (similar in shape, color, and number, but not in shading). In these examples, the actual color of all figures was blue.

2.3. Statistical analysis

All statistical analyses were performed by using SPSS software (version 8). Whether or not distributions were Gaussian was determined using Leven's test; since data proved to be non-uniformly distributed, non-parametric analysis was used. The performance of each age group was examined using one-way Kruskal–Wallis test, with the Mann–Whitney *U*-test for post hoc comparison. Data are presented as the median.

3. Results

The mCBT converted score is shown as a function of age in Fig. 2A. A significant increase in scores was observed

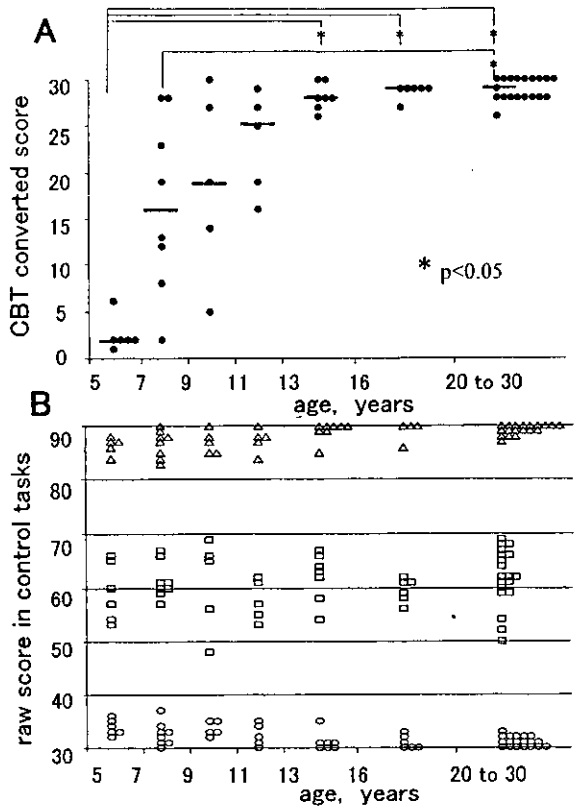

Fig. 2. Converted scores for the modified cognitive bias task (A) and raw scores for control tasks (B) as a function of age. Solid bars represent the median in each age group (5–7 years, 7–9 years, 9–11 years, 11–13 years, 13–16 years, 16–20 years, and 20–30 years). Δ, 'most similar' choice requested; □, 'random' choice (no target); ○, 'most different' choice requested.

with age (Spearman, $r = 0.619$, $P < 0.01$). Scores in children between 7 and 13 years of age showed much greater interindividual variation than those in other age groups. The youngest children (5–7 years) had a lower converted score than other groups aged from 11 years to adulthood (Kruskal–Wallis, $x^2 = 32.05$, $P < 0.01$; Mann–Whitney U-test with Bonferroni correction, $P < 0.05$ vs. groups over 13 years old). Beginning between 7 and 9 years, scores increased as a function of age to reach adult levels by age 13–16. We confirmed that all subjects were able to discriminate the four dichotomies in the two control tasks and showed, by design, a middle-range raw score (around 60) in the task without presentation of a target (Fig. 2B).

4. Discussion

Understanding how the human mind deals with internal or external stimuli to result in behavior remains a major challenge for science [13]. Information processing is a key cognitive link between perception and action [14,15]. Hemispheric specialization in the frontal lobes is hypothesized to exist for cognitive activities (context-dependent vs. context-independent reasoning) in response to ongoing events [7,8,16,17]. The CBT designed by Goldberg et al. in 1994 is one of very few instruments that can directly demonstrate hemispheric specialization in the frontal lobes [9]. Our study therefore is relevant to understanding the processes of mental development as well as impairment of frontal lobe function in children.

4.1. Why focus on right-handed males?

In our preliminary study in adults, one-way Kruskal–Wallis analysis of variance for Cognitive Bias Score showed highly significant differences ($x^2 = 6.637$, $P = 0.036$) between right-handed men ($n = 19$), right-handed women ($n = 13$), and non-right-handed men ($n = 9$; mean ranks, 26.08, 16.27, and 17.11, respectively), as we reported previously [9]. Furthermore, cognitive [18], lesional [9,10], hormonal [19], biochemical [20] evidence indicates that hemispheric specialization is pronounced in right-handed males. For these reasons we focused on right-handed male subjects.

4.2. Details of experimental design for demonstrating hemispheric specialization in the frontal lobes

Traditional intelligence tests measure convergent thinking in the sense that a question usually has just one answer. Tests of divergent thinking, in contrast, emphasize number and variety of answers to a single question [21]. The latter mode of thinking has been reported to be particularly affected by frontal lobe injuries [9,22,23]. In our study, two of the control tasks (selection of the most similar or different choice) demanded convergent thinking. On the other hand, the first task (CBT) required divergent thinking, since bias or preference rather than performance or accuracy was examined. The prefrontal cortex is instrumental in selecting goal-appropriate internal representations and bringing them 'on line' [24]. Left and right prefrontal systems, respectively, show different response selection biases: those guiding behavior relying on internal context-based principles, and those using external environment-based principles [9–11]. If subjects prefer choices more similar to a target, they are deciding based on an internal context of ordering hypothesized to involve the left prefrontal cortex in right-handed men.

According to this hypothesis, the task was designed to ensure that similarity indices for the two choices presented were never equal; therefore, in each trial the subjects had to choose the image more similar to the target or the image more different from the target. Thirty independent, counterbalanced trials were performed, and each subject performed the same sequence of trials. All similarity indexes and unequal target-choice similarity-index pairs were equally represented and counterbalanced throughout the trial sequence.

4.3. Why modify the original CBT?

The original CBT, as described by Goldberg et al. in 1994, entails geometric designs characterized by five variables: color, shape, number, shading, and size (large vs. small). However, we found that young children aged from 5 to 7 could not discriminate all five variables in the two control tasks when explicit instructions were given to choose the figure more similar or different from the target. Accordingly, a computer-administered mCBT was designed for children using four dichotomous variables (color, shape, number, and shading). We confirmed that all subjects were able to discriminate the four dichotomies in the above two control tasks performed after the CBT.

4.4. Why did the degree of left-hemispheric advantage (or context-dependent reasoning) increase with age in these subjects?

We could not rigorously determine whether the timetable for development of hemispheric specialization during childhood depended upon social as opposed to biologic factors, since all Japanese children over 6 years of age have begun compulsory education. Cognitive longitudinal studies [25–27] have indicated that the right hemisphere plays a role in the early stage of learning, and the left-hemisphere takes over at a more advanced learning stage. In an mCBT study in adults, on the other hand, we found both sexual dimorphism and a gender-handedness interaction in neural mechanisms of response selection. This indicates the importance of biologic factors, as seen in Goldberg's studies [9,10]. Further studies using mCBT are needed to examine interactions between gender and handedness as a function of age.

4.5. Clinical significance

In a review of frontal lobe injury during childhood, Anderson et al. postulated that children with frontal lobe lesions are likely to present a globally depressed cognitive profile because of the impact of such injuries on children's capacity to acquire new skills [28]. Therefore, hypothesis-driven studies could contribute to advancements in assessment of frontal lobe dysfunction during childhood. Indeed, our own unpublished mCBT data in patients with unilateral frontal lobe lesions ($n = 15$) or frontal lobe epilepsy ($n = 12$) suggest that extreme context-independent response biases occur in patients with left frontal lobe damage.

Many researchers have concluded that ADHD is caused by a lag in neural development, possibly involving the prefrontal cortex [4,29,30]. Evidence of abnormal left-hemispheric development in another disorder, autism, comes from a study comparing hemispheric specialization for processing of spoken stimuli with that for other stimuli [31], and also from a positron emission tomographic study involving a 'theory of mind' task [32]. We ultimately seek to determine whether a specific relationship exists between abnormal development of hemispheric specialization and pathogenesis in developmental disorders (such as autism, ADHD, and other learning disorders), as previously has been investigated with respect to psychiatric disorders [33].

5. Conclusion

The youngest children in our study displayed extremely context-independent responses, while adolescents and adults responded in an extremely context-dependent manner. This pattern supports the hypotheses that the locus of cortical control in right-handed male subjects shifts from the right to left frontal lobe as cognitive contextual reasoning develops.

Further mCBT studies are needed to examine possible interaction between gender and handedness as a function of age, and to identify the functional anatomy linked to context-dependent reasoning using neuroimaging of activation. Additionally, similar studies in children with ADHD and autistic disorder may shed light on basic questions regarding the effects of a deficit in normal development of hemispheric specialization upon symptoms.

Acknowledgements

Our research was supported in part by The Japan Epilepsy Research Foundation (M.A.).

References

[1] Fuster JM. The prefrontal cortex: anatomy, physiology, and neuropsychology of the frontal lobe, 3rd ed. The prefrontal cortex: anatomy, physiology, and neuropsychology of the frontal lobe. 3rd. Philadelphia: Lippincott-Raven; 1997.
[2] Stuss DT, Knight RT, editors. Principles of frontal lobe function. New York: Oxford University Press; 2002.
[3] Dobbing J, Sands J. Vulnerability of developing brain: the effect of nutritional growth retardation on the timing of the brain growth spurt. Biol Neonate 1971;19:363–78.
[4] Barkley RA, Grodzinsky G. Are tests of frontal lobe function useful in the diagnosis of attention deficit disorders? Clin Neuropsychol 1994; 8:121–39.
[5] Anderson SW, Bechara A, Damasio H, Tranel D, Damasio AR. Impairment of social and moral behavior related to early damage in human prefrontal cortex. Nat. Neurosci 1999;2:1032–7.
[6] Goldberg E, Costa LD. Hemispheric differences in the acquisition and use of descriptive systems. Brain Lang 1981;14:144–73.
[7] Petrides M, Milner B. Deficits on subject-ordered tasks after frontal- and temporal-lobe lesions in man. Neuropsychologia 1982;20: 249–62.
[8] Milner B, Petrides M. Behavioural effects of frontal lobe lesions in man. Trends Neurosci 1984;7:403–7.
[9] Goldberg E, Podell K, Harner R, Riggio S, Lovell M. Cognitive bias, functional cortical geometry, and the frontal lobes: laterality, sex, and handedness. J Cognit Neurosci 1994;6:276–96.

[10] Goldberg E, Podell K. Lateralization in the frontal lobes. In: Jasper HH, Riggio S, Goldman-Rakic PS, editors. Epilepsy and the functional anatomy of the frontal lobe. New York: Raven; 1995. p. 85–96.
[11] Podell K, Lovell M, Zimmerman M, Goldberg G. The cognitive bias task and lateralized frontal lobe functions in males. J Neuropsychiatry Clin Neurosci 1995;7:491–501.
[12] Chapman LJ, Chapman JP. The measurement of handedness. Brain Cogn 1987;6:175–83.
[13] Nichols MJ, Newsome WT. The neurobiology of cognition. Nature (Suppl) 1999;402:35–8.
[14] D'Esposito M, Ballard D, Zarahn E, Aguirre GK. The role of prefrontal cortex in sensory memory and motor preparation: an event-related fMRI study. Neuroimage 2000;11:400–8.
[15] Fuster JM, Bondner M, Kroger JK. Cross-modal and cross-temporal association in neurons of frontal cortex. Nature 2000;405:347–51.
[16] Lhermitte F. 'Utilization behavior' and its relation to lesions of the frontal lobes. Brain 1983;106:237–55.
[17] McCarthy RA, Warrington EK. Cognitive neuropsychology. New York: Academic Press; 1990.
[18] Brydden MP. Tachistoscopic recognition, handedness, and cerebral dominance. Neuropsychologia 1965;3:1–8.
[19] Geschwind N, Galaburda AM. Cerebral lateralization: biological mechanisms, associations and pathology. Cambridge, MA: MIT, Cambridge, MA: MIT Press; 1987.
[20] Tucker DM, Williamson PA. Asymmetric neural control systems in human self-regulation. Psychol Rev 1984;91:185–215.
[21] Milner B. Aspects of human frontal lobe function. In: Jasper HH, Riggio S, Goldman-Rakic PS, editors. Epilepsy and the functional anatomy of the frontal lobe. New York: Raven; 1995. p. 67–84.
[22] Milner B. Effects of different brain lesions on card sorting. Arch Neurol 1963;9:90–100.
[23] Shimamura AP, Janowsky JS, Squire LR. Memory of the temporal order of events in patients with frontal-lobe lesions and amnestic patients. Neuropsychologia 1990;28:803–13.
[24] Goldman-Rakic PS. Circuitry of primate prefrontal cortex and representation of behavior by representational memory. In: Plum VF, editor. Handbook of physiology: the nervous system. Baltimore, MD: American Physiological Society; 1987. p. 373–417.
[25] Miller LK, Turner S. Development of hemifield differences in word recognition. J Educ Psychol 1973;65:172–6.
[26] Carmon A, Nachson I, Starinsky R. Developmental aspects of visual hemifield differences in perception of verbal material. Brain Lang 1976;3:463–9.
[27] Kitter P, Turkewitz G, Goldberg E. Shifts in hemispheric advantage during familiarization with complex visual patterns. Cortex 1978;14: 511–20.
[28] Anderson V, Levin HS, Jacobs R. Executive functions of the frontal lobe injury: a developmental perspective. In: Stuss DT, Knight RT, editors. Principles of frontal lobe function. New York: Oxford University Press; 2002. p. 504–27.
[29] Gorenstein EE, Mammato CA, Sandy JM. Performance of inattentive-overactive children on selected measures of prefrontal-type function. J Clin Psychol 1989;45:619–32.
[30] Swanson J, Castellanos FX, Murias M, LaHoste G, Kennedy J. Cognitive neuroscience of attention deficit hyperactivity disorder and hyperkinetic disorder. Neurobiology 1998;8:263–71.
[31] Dawson G, Finley C, Phillips S, Galpert L. Hemispheric specialization and the language abilities of autistic children. Child Dev 1986; 57:1440–53.
[32] Happe F, Ehlers S, Fletcher P, Frith U, Johansson M, Gillberg C, et al. 'Theory of mind' in the brain. Evidence from a PET scan study of Asperger syndrome. Neuroreport 1996;8:197–201.
[33] Stratta P, Daneluzzo E, Bustini M, Prosperini PL, Rossi A. Schizophrenic patients use context-independent reasoning more often than context-dependent reasoning as measured by the Cognitive Bias Task (CBT): a controlled study. Schizophrenic Res 1999;37: 45–51.

ELSEVIER

Cancer Genetics and Cytogenetics 146 (2003) 102–109

Cancer Genetics and Cytogenetics

Newly established Askin tumor cell line and overexpression of focal adhesion kinase in Ewing sarcoma family of tumors cell lines

Hiroshi Moritake[a,*], Tohru Sugimoto[b], Hiroshi Kuroda[c], Fumio Hidaka[a], Yukiko Takahashi[d], Masazumi Tsuneyoshi[d], Mitsuaki A. Yoshida[e], Qingping Cui[e], Kensuke Akiyoshi[f], Tatsuro Izumi[f], Hiroyuki Nunoi[a]

[a]*Department of Pediatrics, Miyazaki Medical College, Kiyotake, Miyazaki, Japan*
[b]*Department of Pediatrics, Kyoto Prefecture Medical University, Kyoto, Japan*
[c]*Department of Pediatrics, Kyoto City Hospital, Kyoto, Japan*
[d]*Department of Anatomic Pathology, Pathological Sciences, Graduate School of Medical Sciences, Kyushu University, Fukuoka, Japan*
[e]*Laboratory of Molecular Cytogenetics, Department of Chemotherapy, Institute for Clinical Research, National Kyushu Cancer Center, Fukuoka, Japan*
[f]*Department of Pediatrics, Oita Medical University, Oita, Japan*

Received 2 October 2002; received in revised form 3 March 2003; accepted 14 March 2003

Abstract Askin tumor is a malignant small round cell tumor that originates from the thoracopulmonary region and is a member of Ewing sarcoma family of tumors (ESFT). Only a few Askin tumor cell lines have been established. An Askin tumor cell line, designated MP-ASKIN-SA, was established from the left thoracic tumor of a 13-year-old Japanese boy. ESFT is known to have a high rate of distant metastases at diagnosis. The genes controlling the spread of ESFT cells, however, have not been elucidated. G-banding chromosome analysis revealed that the MP-ASKIN-SA cell line has complex chromosomal abnormalities including trisomy 8. The *EWS/FLI1* chimeric transcript and c-myc overexpression were revealed by the reverse transcriptase-polymerase chain reaction and Northern blot analysis. Furthermore, we investigated the expression of the focal adhesion kinase (*FAK*) gene in the ESFT cell lines using Northern blot analysis. In addition to the MP-ASKIN-SA cell line, six Ewing sarcoma cell lines, one peripheral nerve sheath tumor cell line, and two Askin tumor cell lines were analyzed. All ESFT cell lines, including MP-ASKIN-SA, expressed five- to twenty-eight-fold–increased values of *FAK*, as compared with fibroblasts obtained from the bone marrow of a healthy volunteer. These results raise the possibility that the overexpression of *c-myc* and *FAK* are involved in the poor prognosis of ESFT.

1. Introduction

The Ewing sarcoma family of tumors (ESFT) represents small round cell childhood malignancies of bone and soft tissues, and includes Ewing sarcoma (ES), peripheral primitive neuroectodermal tumors, and Askin tumors. Askin tumor, also known as malignant small round cell tumor of the thoracopulmonary region, was originally proposed as a distinct clinicopathologic entity by Askin et al. [1]. This tumor arises in the periosteum, soft tissue, and extrapulmonary fields of the thoracic wall and in the lung, with or without rib involvement, which presents in both children and young adults. Histologically, it contains homogeneous small round-to-spindle cells growing in compact sheets on pseudolobules and is mostly devoid of any particular microscopic differentiation. Rosette-like figures of the Homer-Wright type, however, are occasionally seen. Clinically, tumors of this type resemble those described in bone and soft tissue but they are located anatomically outside the trunk. Local recurrence and metastasis are observed frequently, leading to poor survival rates.

Cytogenetically, most tumors in the ESFT share the same reciprocal t(11;22)(q24;q12) or t(21;22)(q22;q12) [2,3]. These chromosomal translocations result in a fusion protein of the N-terminal EWS region and the C-terminal FLI1 or ERG region [2,3]. The *EWS/FLI1* protein has been shown to transform NIH3T3 cells efficiently and is thought to be involved in the oncogenesis of ESFT [4].

* Corresponding author. Department of Pediatrics, Miyazaki Medical College, 5200 Kihara, Kiyotake, Miyazaki 889-1692, Japan. Tel.: +81-985-85-0989; fax: +81-985-85-2403.
E-mail address: moritake@fc.miyazkai-med.ac.jp (H. Moritake).

0165-4608/03/$ – see front matter
doi: 10.1016/S0165-4608(03)00129-8

[44] Haniu M, McManus ME, Birkett DJ, Lee TD, Shively JE. Structural and functional analysis of NADPH-cytochrome P-450 reductase from human liver: complete sequence of human enzyme and NADPH-binding sites. Biochemistry 1989;28:8639–45.

[45] Bustamante J, Bersier G, Badin RA, Cymeryng C, Parodi A, Boveris A. Sequential NO production by mitochondria and endoplasmic reticulum during induced apoptosis. Nitric Oxide 2002;6:333–41.

[46] Waxman DJ, Chen L, Hecht JE, Jounaidi Y. Cytochrome P450-based cancer gene therapy: recent advances and future prospects. Drug Metab Rev 1999;31:503–22.

[47] Harris CC, Hollstein M. Clinical implications of the p53 tumor-suppressor gene. N Engl J Med 1993;329:1318–27.

[48] Levine AJ, Momand J, Finlay CA. The p53 tumor suppressor gene. Nature 1991;351:453–6.

[49] Fenaux BP, Jonveaux P, Quiquandon I, Lai JL, Pignon JM, Locheux-Lefebvre MH, Bauters F, Berger R, Kerckaert JP. P53 mutations in acute myeloid leukemia with 17p monosomy. Blood 1991;78:1652–7.

[50] Hu G, Zhang W, Deisseroth AB. P53 gene mutations in acute myelogenous leukaemia. Br J Haematol 1992;81:489–94.

[51] Schottelius A, Brennscheidt U, Ludwig W-D, Mertelsmann RH, Herrmann F, Lübbert M. Mechanisms of p53 alteration in acute leukemias. Leukemia 1994;8:1673–81.

[52] Brinkmann U, Brinkmann E, Gallo M, Pastan I. Cloning and characterization of a cellular apoptosis susceptibility gene, the human homologue to the yeast chromosome segregation gene CSE1. Proc Natl Acad Sci USA 1995;92:10427–31.

[53] Smith ML, Chen IT, Zhang Q, Bae I, Chen CY, Gilmer TM, Kastan MB, O'Connor PM, Fornace AJ Jr. Interaction of the p53-regulated protein Gadd45 with proliferating cell nuclear antigen. Science 1994;266:1376–80.

[54] Takekawa M, Saito H. A family of stress-inducible GADD45-like proteins mediate activation of stress-responsive MTK1/MEKK4 MAPKKK. Cell 1998;95:521–30.

[55] Chin PL, Momand J, Pfeifer GP. In vivo evidence for binding of p53 to consensus binding sites in the p21 and GADD45 genes in response to ionizing radiation. Oncogene 1997;15:87–99.

[56] Santucci MA, Ripalti A, di Paola MC, Mianulli AM, Iacurti E, Campanini F, Gamberi B, Tura S. Procedure for the quantification of Gadd45 expression levels in clonal hematopoietic progenitors cells by competitive polymerase chain reaction. Clin Biochem 1999;32:1–8.

[57] Zhang W, Hoffman B, Liebermann DA. Ectopic expression of MyD118/Gadd45/CR6 (Gadd45beta/alpha/gamma) sensitized neoplastic cells to genotoxic stress-induced apoptosis. Int J Oncol 2001; 18:749–57.

[58] Zhang Y, Xiong Y, Yarbrough WG. ARF promotes MDM2 degradation and stabilizes p53: ARF-INK4a locus deletion impairs both the Rb and p53 tumor suppression pathways. Cell 1998;92:725–34.

[59] Serrano M, Hannon GJ, Beach D. A new regulatory motif in cell-cycle control causing specific inhibition of cyclin D/CDK4. Nature 1993;366:704–7.

[60] Mori T, Miura K, Fujiwara T, Shin S, Inazawa J, Nakamura Y. Isolation and mapping of a human gene (DIFF6) homologous to yeast CDC3, CDC10, CDC11, and CDC12, and mouse Diff6. Cytogenet Cell Genet 1996;73:224–7.

[61] Chang L, Karin M. Mammalian MAP kinase signalling cascades. Nature 2001;410:37–40.

[62] Milella M, Kornblau SM, Estrov Z, Carter BZ, Lapillonne H, Harris D, Konopleva M, Zhao S, Estey E, Andreeff M. Therapeutic targeting of the MEK/MAPK signal transduction module in acute myeloid leukemia. J Clin Invest 2001;108:851–9.

[63] Chen CR, Kang Y, Siegel PM, Massague J. E2F4/5 and p107 as Smad cofactors linking the TGF-beta receptor to c-myc repression. Cell 2002;110:19–32.

[64] Purrello M, Bettuzzi S, Di Pietro C, Mirabile E, Di Blasi M, Rimini R, Grzeschik KH, Ingletti C, Corti A, Sichel G. The gene for SP-40, human homolog of rat sulfated glycoprotein 2, rat clusterin, and rat testosterone-repressed prostate message 2, maps to chromosome 8. Genomics 1991;10:151–6.

[65] Jones SE, Jomary C. Clusterin. Int J Biochem Cell Biol 2002; 34:427–31.

[66] Trougakos I, Gonos E. Clusterin/apolipoprotein J in human aging and cancer. Int J Biochem Cell Biol 2002;34:1430–48.

[67] Schoch C, Kohlmann A, Schnittger S, Brors B, Dugas M, Mergenthaler S, Kern W, Hiddemann W, Eils R, Haferlach T. Acute myeloid leukemias with reciprocal rearrangements can be distinguished by specific gene expression profiles. Proc Natl Acad Sci USA 2002; 99:10008–13.

[68] Pearson LL, Castle BE, Kehry MR. CD40-mediated signaling in monocytic cells: upregulation of tumor necrosis receptor-associated factor mRNA and activation of mitogen-activated protein kinase signaling pathways. Int Immunol 2001;13:273–83.

The genetic aberrations that are responsible for the malignant progression of ESFT, however, are poorly understood. Sollazzo et al. suggested a possible role of the *c-myc* gene in the malignant progression of ES [5]. The *c-myc* gene is related to the malignant progression of various tumors [6]. Another candidate gene is the focal adhesion kinase (*FAK*) gene. *FAK* is a tyrosine kinase that localizes to cellular focal adhesions and associates with a number of other proteins such as integrin adhesion receptors [7]. Studies addressing the role of FAK in cell adhesion suggest that it can contribute to both focal adhesion assembly and focal adhesion turnover [8]. FAK overexpression has been found in various tumors, which suggests that it is related to the malignant progression of these tumors [9–12]. Whether there is a relationship between ESFT and *FAK* overexpression, however, has not yet been examined.

In this study, a new Askin tumor cell line was established from the left thoracic tumor of a 13-year-old Japanese boy. The cell line was characterized and confirmed to have a characteristic phenotype of ESFT, clinically, histologically, and cytogenetically. Furthermore, examination of 10 ESFT cell lines indicated a possible association between *FAK* overexpression and malignant progression of ESFT.

2. Materials and methods

2.1. Clinical history

A 13-year-old Japanese boy was referred to the Oita Medical University in January 1998 with a 3-month history of pain in the left chest. A physical examination revealed an enlarged mass in his left back. A CT scan of the chest showed a huge heterogeneous soft-tissue mass in the left thoracic cavity (Fig. 1). Biopsy of the tumor was composed of a diffuse proliferation of small round cells with hyperchromatic nuclei in small amounts of fibrovascular stroma. The tumor cells showed scant or clear cytoplasm (Fig. 2A). Most of the tumor cells strongly reacted with HBA71 antibody (Fig. 2B). The tumor was diagnosed as an Askin tumor. Three courses of preoperative chemotherapy with cyclophosphamide (CY), etoposide (VP-16), cisplatin, and pirarubicin,

Fig. 1. Horizontal CT scan of the chest of a 13-year-old boy with a large heterogeneous tumor (13 × 11 × 7 cm) on the left side of the chest cavity.

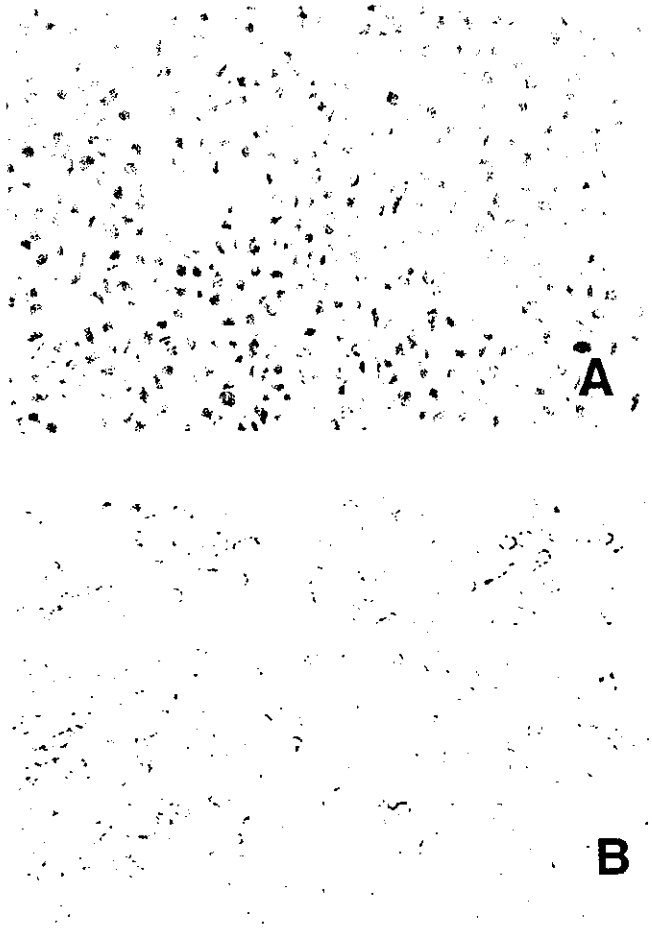

Fig. 2. Histopathologic and immunohistochemical appearance of the primary tumor. (A) A proliferation of small round cells having hyperchromatic nuclei (hematoxylin and eosin; ×400). (B) Most of the tumor cells showed strong positive immunoreactivity with HBA71 antibody.

and complete surgical resection led to a complete response. The patient received an additional two courses of combination chemotherapy with actinomycin D and CY, and three courses of combination chemotherapy with vincristine, pirarubicin, CY, and VP-16, ifosfamide, and irradiation to the left thoracic cavity (5,000 cGy in fractions). In light of his poor prognosis, an autologous bone marrow transplantation was performed in February 1999. In July 1999, routine examination with a computed tomography scan revealed a recurrence in the left thoracic cavity. Despite the subsequent intensive therapy, in May 2000 the patient expired due to progressive disease.

2.2. Cell culture

A tumor sample for cell culture was obtained from the thoracic tumor at the time of recurrence (August 1999). Informed consent for use of the tissue in research was obtained from the patient's parents. The tumor tissue was minced and suspended in RPMI-1640 medium containing penicillin (100 U/mL), streptomycin (100 μg/mL), and 10%

heat-inactivated fetal calf serum. The cultures were incubated at 37°C in a humidified atmosphere of 5% CO_2 in air. The medium was changed every 3–4 days. Upon reaching the confluent state, the monolayers were treated with trypsin and the dispersed cells were transferred into new collagen-coated culture flasks.

2.3. Immunohistochemistry

To test for the expression of HBA71 antigen in a tissue sample, HBA71 monoclonal antibody (Dako Japan, Kyoto, Japan) was used. Tissue was fixed in 10% formalin for 18 hours and embedded in paraffin. Sections (4 μm thick) were examined immunohistochemically with the standard streptavidin-biotin-immunoperoxidase staining method (Histofine SAB-PO kit; Nichirei, Tokyo, Japan). Preimmune mouse IgG was used as a negative control.

2.4. Chromosome analysis

For cytogenetic studies, chromosomes were prepared by standard techniques and analyzed by the Q-banding method as described previously [13].

2.5. Detection of chimeric transcript EWS/FLI1 by reverse transcriptase polymerase chain reaction (RT-PCR)

Total RNA was extracted from cultured cells using a TRIZOL RNA extraction kit (GIBCO BRL, Rockville, MD). An ES cell line, RD-ES, was used as a positive control [14]. A neuroblastoma cell line, KP-N-RT, was used as a negative control [15]. Reverse transcription of 1 μg total RNA was carried out using a reaction mixture of a first-strand cDNA synthesis kit (Takara Shuzo, Kyoto, Japan). The primers for the fusion gene were 5′-CCCACTAGTTACCCACCCCA-3′ for sense and 5′-TGTTGGGCTTGCTTTTCCGCTC-3′ for antisense [2]. After a 60-minute incubation at 37°C, 0.2 μmol/L of each primer and 0.025 U/μL of Taq DNA polymerase were added, and the total volume was adjusted to 50 μL with distilled water. Thermal cycling was performed with an initial denaturation at 94°C for 1 minute, 35 cycles of denaturation at 94°C for 1 minute, annealing at 68°C for 1 minute, and extension at 72°C for 1 minute. The polymerase chain reaction (PCR) products were electrophoresed in a 2% agarose gel in the presence of 0.5 μg/mL ethidium bromide and revealed by ultraviolet irradiation. The *β-actin* gene was also amplified as a control to demonstrate the integrity of the cDNA after PCR.

2.6. Sequencing

Both strands (80 ng PCR product of each) were sequenced using the cycle sequence method with a Prism BigDye Terminator Cycle Sequencing Ready Reaction kit and a model 310 sequencer (both from Applied Biosystems, CA, USA)

2.7. ESFT cell lines

Ten cell lines were used to examine the degree of *FAK* expression in various ESFT cell lines. These included six ES cell lines (KP-EW-YI, KP-EW-MS, RD-ES, SK-ES-1, TC71, and SCMC-ES1), one peripheral nerve sheath tumor cell line (SK-N-LO), and three Askin tumor cell lines (NCR-EW3, SK-N-MC, MP-ASKIN-SA) [14,16–19].

2.8. c-myc *and* FAK *mRNA expressions*

Twenty micrograms of total RNA was electrophoresed through a 1.5% formaldehyde-agarose gel and transferred to a nylon membrane by Northern blotting, as described previously [13]. The membranes were hybridized with a ^{32}P-radiolabeled DNA probe. Each probe of *c-myc* and *FAK* was a 660- and a 1010-base pair (bp) fragment, respectively. The *β-actin* gene was also used as an internal control. The relative intensities of the hybridization signals were quantified by scanning the autoradiograms with a densitometer. For the analysis of c-*myc* expression, the human promyelocytic leukemia cell line HL60, which highly expresses c-*myc*, was used as a positive control [20] and peripheral lymphocytes from a healthy volunteer were used as a negative control. For the analysis of FAK expression, the RD rhabdomyosarcoma cell line, which is known to highly express *FAK*, was used as a positive control [11], and fibroblasts obtained from the bone marrow of a healthy volunteer were used as a negative control. *FAK* expression was also examined in the neuroblastoma cell line SJ-N-KP [21] and in the undifferentiated sarcoma cell line A204 [22] as representative malignant tumors other than ESFT.

3. Results

3.1. Establishment of the MP-ASKIN-SA cell line

Tumor cells obtained from a metastasis of the thoracic cavity grew in the form of an adherent monolayer. The cells have a polygonal shape with processes (Fig. 3). The cells have

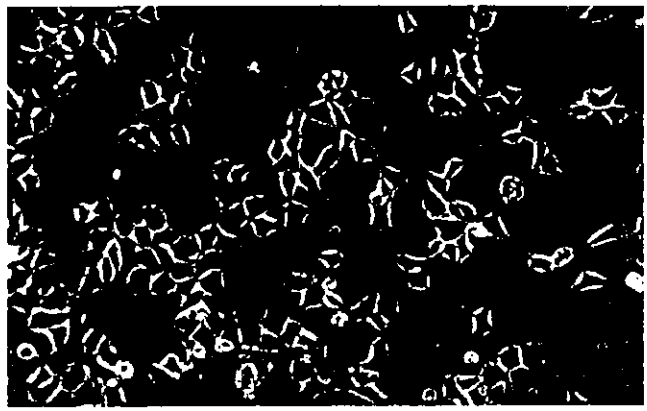

Fig. 3. Phase-contrast microphotograph of the MP-ASKIN-SA cell line. Small polygonal cells with slender processes are shown (×200).

Table 1
Karyotypes of 15 metaphase cells from the MP-ASKIN-SA cell line

Karyotype	No. of cells
50,X,−Y,+1,t(7;12)(p22;q22),+8,del(9)(p22),−11,+12,+15,+20,+22	1
51,X,−Y,+1,t(7;12)(p22;q22),+8,del(9)(p22),add(11)(q22),+12,+15,+20,+22	4
51,X,−Y,+1,t(7;12)(p22;q22),+8,del(9)(p22),add(11)(q22),+12,+13,+22,+mar	1
51,X,−Y,+1,t(7;12)(p22;q22),+8,del(9)(p22),add(11)(q22),+12,+15,+2mars	1
51,X,−Y,+1,t(7;12)(p22;q22),+8,del(9)(p22),−10,add(11)(q22),+12,+15,+20,+22,+mar	1
51,X,−Y,+1,t(7;12)(p22;q22),+8,del(9)(p22),add(11)(q22),+12,+15,+20,+mar	1
51,X,−Y,+1,t(7;12)(p22;q22),+8,−9,del(9)(p22),add(11)(q22),−11,+12,+15,+20,+22,+2mars	1
52,X,−Y,+1,t(7;12)(p22;q22),+8,del(9)(p22),add(11)(q22)2x,+12,+15,+20,+22	1
52,X,−Y,+1,t(7;12)(p22;q22),+8,−9,del(9)(p22),−10,add(11)(q22),+12,+15,+20,+4mars	1
52,X,−Y,+1,t(7;12)(p22;q22),+8,del(9)(p22),add(11)(q22),+12,+15,+20,+22,+mar	1
53,X,−Y,t(7;12)(p22;q22),der(9)t(9;?)(p22;?),−10,add(11)(q22),+12,+13,+15,+20,+5mars	1
58,X,−Y,+1,+2,+5,+6,der(7)t(7;12)(p22;q22),+8,del(9)(p22),add(11)(q22),+12,+13,+14,+15,+16,+18,−19,+20,+21,+mar	1

been maintained for more than 50 passages over a 2-year period. This new cell line was designated MP-ASKIN-SA. The doubling time of the cultured cells is 19 hours.

3.2. Chromosome analysis

For a chromosome analysis, a total of metaphases were examined. The modal chromosome number was 51 and a representative karyotype was 51,X,−Y,+1,t(7;12) (p22;q22), +8,del(9)(p22),add(11)(q22),+12,+15,+20,+22 (Table 1; Fig. 4). The reciprocal t(11;22)(q24;q12), which is a characteristic cytogenetic abnormality of ESFT, was not found.

3.3. Detection of chimeric transcript EWS/FLI1 by RT-PCR

EWS/FLI1 chimeric transcripts were detected in the MP-ASKIN-SA cell line (Fig. 5).

3.4. Sequencing

Sequencing of the amplified cDNA confirmed that EWS exon 7 is fused to FLI1 exon 6 (Fig. 6).

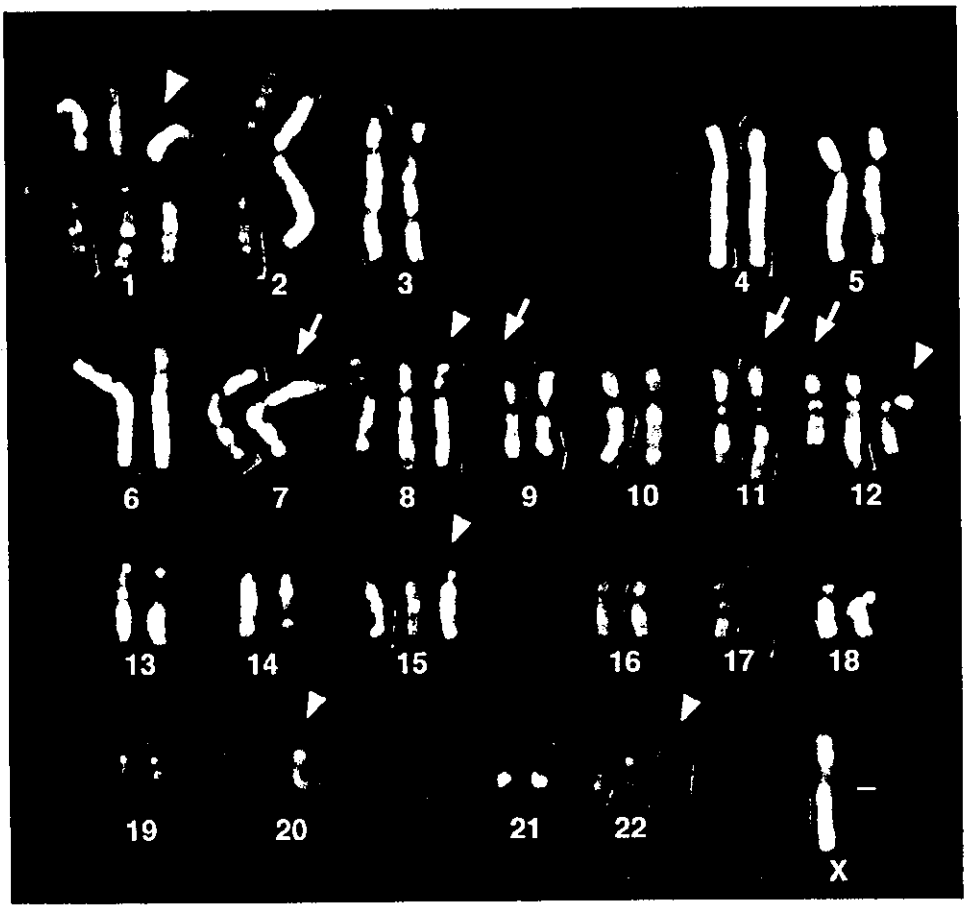

Fig. 4. A representative Q-banded karyotype of the MP-ASKIN-SA cell line: 51,X,−Y,+1,t(7;12)(p22;q22),+8,del(9)(p22),add(11)(q22),+12,+15,+20,+22. Arrows indicate structural abnormalities and arrowheads indicate numerical changes.